Journal of Luminescence 250 (2022) 119035

Contents lists available at ScienceDirect

Journal of Luminescence

journal homepage: www.elsevier.com/locate/jlumin

Fluorescence optimization and ratiometric thermometry of near-infrared emission in erbium/oxygen-doped crystalline silicon

Pu Zhang [a], Jin Hong [b], Huimin Wen [a,*], Hao Wei [a], Jingquan Liu [a], Fangyu Yue [b,**], Yaping Dan [a,c,***]

[a] National Key Laboratory of Science and Technology on Micro/Nano Fabrication Laboratory, Department of Micro/Nano Electronics, School of Electronic Information and Electrical Engineering, Shanghai Jiao Tong University, Shanghai 200240, China

[b] Key Laboratory of Polar Materials and Devices, Ministry of Education, East China Normal University, Shanghai 200241, China

[c] University of Michigan-Shanghai Jiao Tong University Joint Institute, Shanghai Jiao Tong University, Shanghai 200240, China

ARTICLE INFO

Keywords:
Silicon photonics
Erbium
Photoluminescence
Near-infrared emission
Ratiometric thermometry

ABSTRACT

Crystalline Si (c-Si) implanted with rare-earth erbium (Er) might offer a solution to the development of silicon-based optical amplifiers and lasers at communication wavelengths for integrated silicon photonics. However, Er doped (often with oxygen) c-Si traditionally suffers from a strong thermal quenching effect in luminescence, resulting in extremely low luminous efficiency. We recently adopted a deep cooling process to treat Er/O co-doped c-Si samples. After the treatment, the thermal quenching effect is suppressed and the room-temperature photoluminescence (PL) is improved by two orders of magnitude. In this work, we report the PL optimization by tuning parameters including annealing temperature and time, deep cooling rate, O and Er concentration, and their ratio. It was found that the PL performance is maximized at O:Er concentration ratio of ~2.5 and annealing temperature of 950 °C for 5 min followed by a cooling rate as fast as −500 °C s^{-1}. In addition, the Er/O emission has two spectrally-resolved peaks at 6472 cm^{-1} and 6510 cm^{-1} and their intensity ratio is independent of excitation power but a linear function of temperature. This unique property, likely originated from the physics of Er, Si, and O chemical composites formed in the deep cooling process, allows us to develop reliable cryogenic temperature sensors with an accuracy of ±1.0 K in the 4–200 K range.

1. Introduction

The evolution of silicon photonics as an emerging technology for optical interconnection requires the monolithic integration of on-chip light sources with complementary metal-oxide-semiconductor (CMOS) circuits [1–5]. Crystalline silicon (c-Si) is a de facto inefficient emitter of light owing to its indirect bandgap. Alternatively, erbium ions (Er^{3+}) have radiative emissions at 1.54 μm, arising from an intra-4*f* transition between $^4I_{13/2}$ and $^4I_{15/2}$ and lighting upon the low-loss windows for fiber optic communications. Introducing Er into silicon was hence believed to be a promising approach to creating silicon-based light--emitting sources [6–10]. During the past four decades, photoluminescence (PL) and electroluminescence from Er-doped silicon obtained by molecular beam epitaxy and ion implantation have been extensively investigated [11–14]. As a nonequilibrium method, high-dose ion implantation can bring typical erbium densities up to 10^{-21} cm^{-3}, far beyond its solubility limit, while posing a lot of crystalline damages in silicon that leads to the non-radiative paths for electron-hole pair recombination and severely affects the luminescence efficiencies of Er-implanted materials [15,16]. In spite of a standard rapid thermal annealing at high temperature to heal these damages, there is not yet a strong emission of light for erbium in intrinsic silicon matrices [9,13,17,18].

Recently, our research group has reported a two-order-of-magnitude improvement in PL intensity for Er-doped silicon devices, with an external quantum efficiency achieving 0.8% at room temperature, as a result of suppressing the segregation of Er-related precipitates by deep cooling (DC) process [11,12]. In this work, the impact of critical DC

* Corresponding author.
** Corresponding author.
*** Corresponding author. National Key Laboratory of Science and Technology on Micro/Nano Fabrication Laboratory, Department of Micro/Nano Electronics, School of Electronic Information and Electrical Engineering, Shanghai Jiao Tong University, Shanghai 200240, China.
E-mail addresses: wenhuimin@sjtu.edu.cn (H. Wen), fyyue@ee.ecnu.edu.cn (F. Yue), yaping.dan@sjtu.edu.cn (Y. Dan).

https://doi.org/10.1016/j.jlumin.2022.119035
Received 11 October 2021; Received in revised form 22 April 2022; Accepted 27 May 2022
Available online 3 June 2022

parameters including annealing temperature and time as well as cooling rate was systematically investigated. PL results indicate that the Er-doped c-Si samples annealed at 950 °C for 5 min and then cooled down with a rate of -500 °C·s^{-1} have a maximum near-infrared (NIR) emission. The PL results was further optimized by tuning the O:Er concentration ratio to 2.5. Based on the stark splitting of $^4I_{15/2}$ and $^4I_{13/2}$ levels, a representative fluorescence ratiometric thermometry at cryogenic temperatures down to 4 K has been developed for these Er/O-doped silicon phosphor materials. By using the linear equation derived from the temperature-dependent regression analysis of two intensity ratio at 6472 cm^{-1} and 6510 cm^{-1}, the read-out temperature fully agrees with the preset values with a precision in the measurement of ±1.0 K, pointing the way for fabricating the integrated cryogenic temperature sensors in rare-earth-doped silicon [19–22].

2. Materials and methods

Float zone intrinsic Si (100) wafers (resistivity: ≥ 10 kΩ cm; thickness: 500 ± 20 μm) were purchased from commercial sources (Suzhou Resemi Semiconductor Co., Ltd). The as-received wafer was implanted by different O ion concentrations between 4×10^{19} cm^{-3} and 2×10^{21} cm^{-3}, with an injection energy of ~32 keV (Institute of Semiconductors, Chinese Academy of Sciences). Subsequently, multiple Er ion concentrations in the 10^{19} - 10^{21} cm^{-3} range were chosen to implant, in accordance with the O:Er concentration ratios of 0.05, 0.25, 0.5, 1.5, 2.5, and 3.5, respectively. The Er injection energy was ~200 keV, enabling a peak depth of about 80 nm, similar to that of O ions in silicon. These implantation parameters, used to suitably form a comparable Er/O doping profile, were provided by SRIM software [23,24]. After that, the as-implanted Si samples were cleaned with ethanol and deionized water, and then immersed in a piranha solution (sulfuric acid: 30% hydrogen peroxide = 3:1) for 30 min at 90 °C, followed by drying with a high purity nitrogen (99.99%) stream. A 200-nm-thick SiO_2 films was then deposited on the Er/O-implanted Si samples by reactive magnetron sputtering (Delton multi-target magnetic control sputtering system, AEMD, SJTU). Finally, a deep cooling process was performed to activate Er optical centers and to repair silicon lattice via an upgraded dilatometer (DIL 805A, TA Instruments), where the samples were annealed at 800 °C–1100 °C by means of copper coil-based electromagnetic heating and followed by a flush of high purity He (99.999%) gas cooled in liquid N_2 (77 K). Similar procedures for Er/O-doped Si samples can be referred to our previous descriptions [11,12].

For PL characterizations, a Fourier transform infrared (FTIR) spectrometer (Vertex 80v, Bruker) was employed. The focused 405-nm emission from a continuous-wave laser (MLL–III–405, CNI) with a maximum pump power of ~160 mW was used as the excitation source. Notch, neutral density, and long-pass filters were utilized for avoiding the influence of the excitation during the excitation power dependent PL measurements [25]. Temperature read-out experiments were carried out in order to determine the temperature reliability and accuracy related to the Er/O-doped silicon thermometry. It was implemented by mW-excitation with a 405-nm laser diode being operated at less than ~100 mW, a high-performance Ge photodiode, a cube beam splitter with a 10:90 (R:T) split ratio for 1100–1600 nm (BS045, Thorlabs), and a home-built temperature control system (Lakeshore 335 and Cryocon 22C) for presetting and controlling temperature. In all measurements the samples were mounted on the cold head of a Helium closed cycle cooler. This allows for temperature adjustment from 4 K to ambient.

3. Results and discussion

3.1. Optimization of deep cooling process

As previously pointed out, the DC treatment can improve the PL efficiency of Er/O-doped silicon by nearly two orders of magnitude, in comparison with the standard rapid thermal annealing [12]. To further optimize it, we first annealed the Er/O-implanted silicon samples at different temperatures in the range of 800–1100 °C. PL spectra were then characterized with high-resolution FTIR spectrometer by using a 405-nm diode laser as light source. The results indicate that the PL intensity, featuring a main peak at 1536 nm (6510 cm^{-1}), rises by an order of magnitude when the annealing temperature increases from 800 °C to 950 °C, as shown in Fig. 1 (a) and (b). Further increase in temperature will significantly quench the PL. This trend is similar to the literature reports [26,27]. The decrease in luminescence beyond 950 °C is ascribed to the dissociation of Er–O radiative centers [26,27]. It thus suggests there is a critical annealing temperature at 950 °C that benefits the NIR emission for our Er/O-doped silicon. At this critical temperature, we also extended the annealing time from 0.5 min to 30 min. Fig. 1 (c) and (d) show that an annealing duration of 5 min can produce a relatively more intensified PL for Er/O-doped silicon.

Note that the improvement of luminescence efficiency of Er/O co-doped Si samples was attributed to the suppression of the precipitation of Er/O-related composites, as discussed in our previous works [11,12]. Therefore, the cooling rate should have a significant impact on the PL intensity of Er/O-doped silicon. For this reason, we ramped up the cooling rate by increasing the flow rate of He gas from 100 mL s^{-1} to 300 mL s^{-1}. As observed in Fig. 1 (e) and (f), the PL intensity of Er-doped silicon experiences a monotonous growth when the cooling rate accelerates to -500 °C s^{-1}. The timely cooling process suppresses the growth of Er_2O_3/$ErSi_{1.7}$ precipitations, resulting in a strong room-temperature PL emission at 1.54 μm from the samples [12]. It is noted that the samples can be cooled sharply to room temperature in less than 2 s via our upgraded dilatometer. In view of this, if processed properly, the samples might emit more powerfully by means of other cooling procedures at nanosecond level, such as excimer laser annealing [28].

3.2. The concentration and ratio of Er and O dopants

According to Kimerling (1991, Reference [29]) and Kenyon (2005, Reference [9]), co-doping with some electronegative impurities such as carbon, oxygen, or fluorine can improve the spectral performance by providing a solvation environment around Er^{3+} ions. In this work, O and Er dopants with six different ratios from 0.05 to 3.5 were implanted (see the section of Materials and methods). After DC treatment, the measured PL results were analysed in Fig. 2 (a). It indicates that the PL intensity increases steadily as the O:Er ratio rises from 0.05 to 2.5. After that, there is an unexpected reduction at 3.5. Clearly, the optimal O:Er concentration ratio is ~2.5, a little higher than the results in SOI samples [13].

To map the spatial distribution of Er and O elements in crystalline silicon, atom probe tomography (APT) was performed in a Cameca LEAP 4000X SI in laser mode with the following parameters: temperature 20 K, pulse repetition rate 200 kHz, laser energy 40 pJ, and target evaporation rate 0.5%. The APT analysis shows that the exact O:Er ratio is approximately 1.5, less than the nominal value of 2.5, due to the aggregation of Er atoms [12]. It suggests that Er binds with O in the form of Er_2O_3-like composites, resulting in the strongest light emission at 1.54 μm. Since the concentration of Er dopants also has a significant impact on the PL properties, samples with Er concentrations between 8.0×10^{19} cm^{-3} and 1.2×10^{21} cm^{-3} were further investigated. Despite having a different O:Er concentration ratio (1.5:1, blue dots and 2.5:1, red dots in Fig. 2 (b)), both curves reached a peak of PL intensity at an identical Er concentration of 8.0×10^{20} cm^{-3}, far beyond the solubility limit of Er in silicon.

3.3. Temperature- and excitation power-dependent PL

To understand the luminescence mechanism of DC-processed samples, temperature- and excitation power-dependent PL measurements were further conducted (see the section of Materials and methods). Fig. 3 (a) is the PL spectra of Er/O-doped silicon at increasing

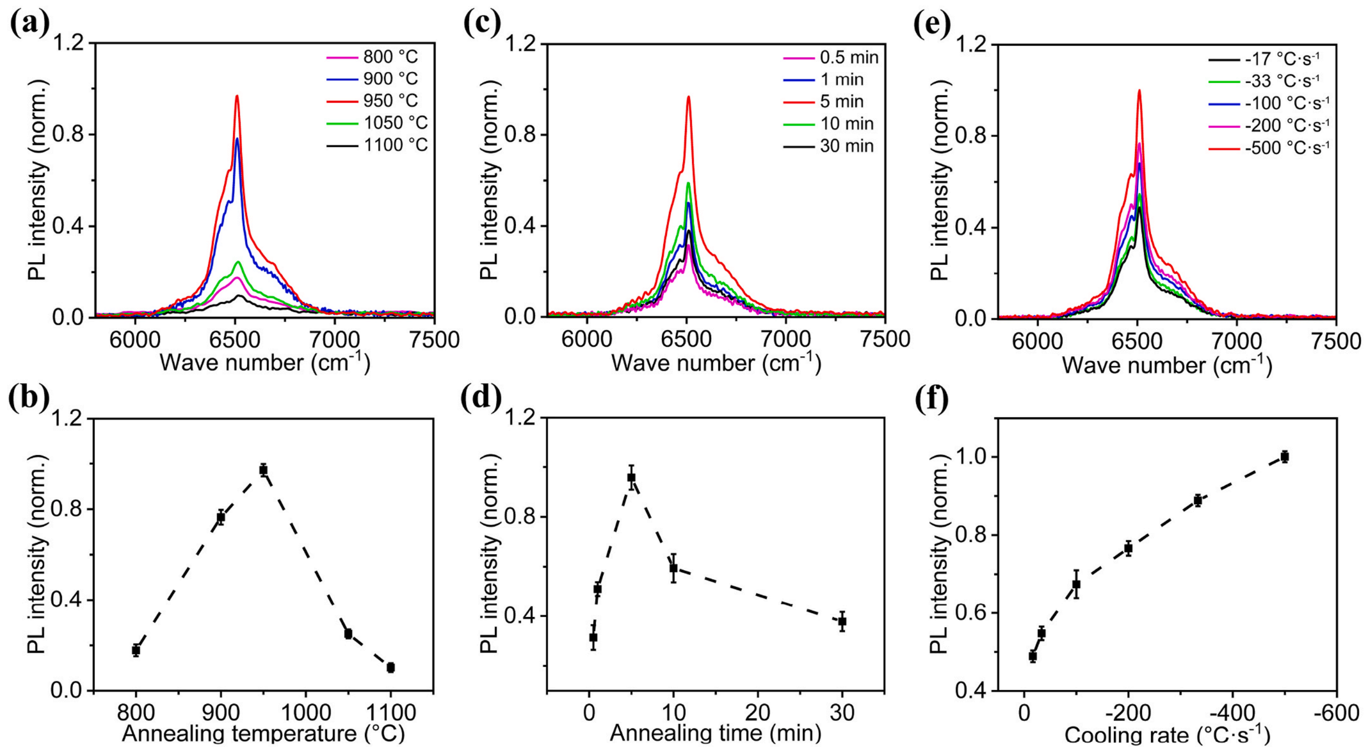

Fig. 1. (a) PL spectra and (b) peak intensity at 6510 cm^{-1} of Er/O-doped silicon treated with different annealing temperatures, (c) and (d) different annealing times, and (e) and (f) different cooling rates. In (b), (d), and (f), each data point is presented as average ± standard deviation from three independent samples, and the dash lines are guides for the eye.

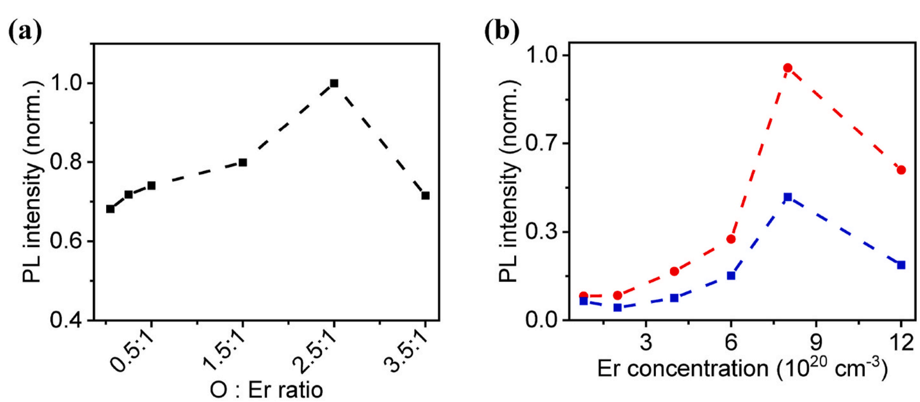

Fig. 2. PL intensity at 6510 cm^{-1}, measured at 300 K, of Er/O-doped silicon as a function of (a) O:Er ratio (black squares) and (b) Er concentration (blue squares, O:Er = 1.5 : 1; red dots, O:Er = 2.5 : 1). In both (a) and (b), the dash lines are guides for the eye.

temperature from 4 K to 300 K. It is well known that the emission originating from an intra-4*f* transition of Er has nearly no shift in wavelength no matter how the surrounding temperature changes. As shown in Fig. 3 (a), the PL maximum of Er/O-doped silicon is merely located at 6510 cm^{-1} (1536 nm, peak 1), despite a seven-fold thermal quenching of its intensity as temperature increases from 4 K to 300 K. Notably, there is always a resolved shoulder at 6472 cm^{-1} (1545 nm, peak 2) in all PL spectra. Referring to Hughes et al. [30], a total of 17 peaks including hot lines from the Er-related cubic and non-cubic symmetry centers had been identified between 6000 cm^{-1} and 6750 cm^{-1}. As for our Er/O-doped Si samples, almost a comparable amount of peaks can be accordingly fitted out with Gaussian functions [31,32], among which two diverse ones at 6472 cm^{-1} and 6510 cm^{-1} can be attributed to the O coordinated Er center with non-cubic symmetry (Fig. 3 (b)).

As the laser pump power ramps up from 0.1 mW to 100 mW, the PL intensity of Er/O-doped Si increases as illustrated in Fig. 3 (c). When the integrated intensity of peaks 1 and 2 are separately plotted versus excitation power in Fig. 3 (d), both curves are sublinearly dependent on the excitation power ($I_{PL} \propto P^{0.6}$) in the low power regime, owing to the impurity- or defect-related emission in Er/O-doped silicon [9]. What is more important, these two curves are parallel in the low power range, making their intensity ratio independent of the excitation power [33, 34].

3.4. Fluorescence ratiometric thermometries

The aforementioned fact that the intensity ratio of peaks 1 and 2 are independent of the excitation power is reasonable, because these two peaks are the transition from the $^4I_{13/2}$ manifold of Er ions due to stark splitting. The ratio of their intensity is determined by how excitons statistically distribute among them, which is governed by the Boltzmann

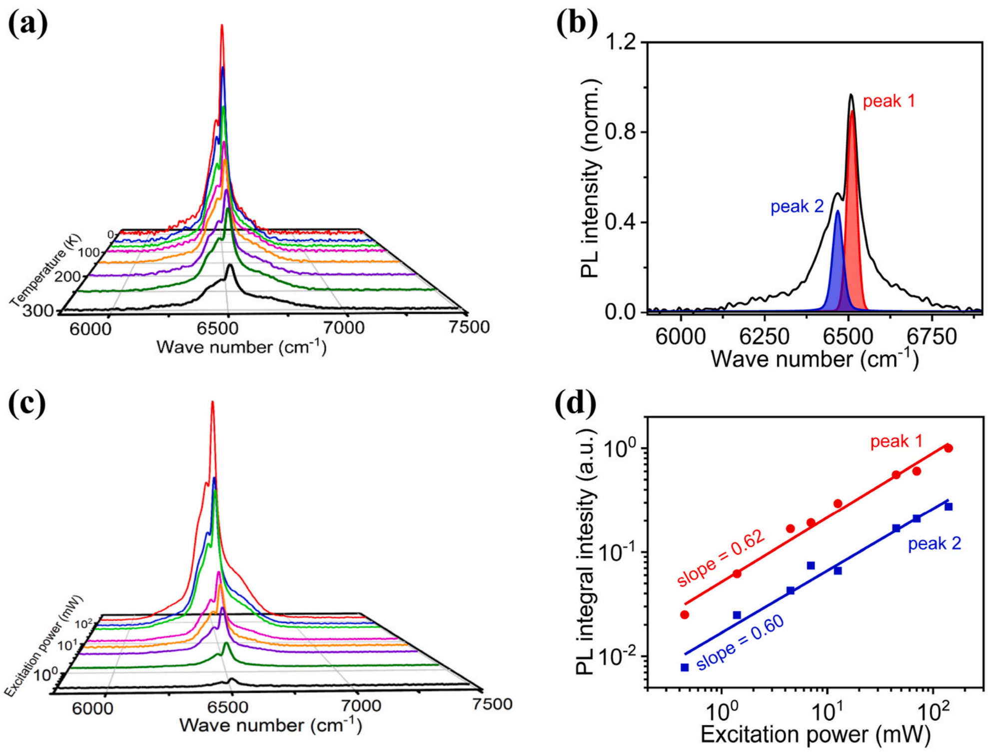

Fig. 3. (a) Temperature-dependent PL spectra of Er/O–Si samples. (b) The Gaussian function fitting of PL results (black line) at 300 K. The fitting components are two resolved peaks of 6472 cm^{-1} (blue line) and 6510 cm^{-1} (red line), respectively. (c) Excitation power-dependent PL spectra of Er/O–Si samples. (d) Integrated PL intensity vs. excitation power of the 405-nm laser at 6472 cm^{-1} (blue squares) and 6510 cm^{-1} (red dots), respectively. The red and blue solid lines are the linear fits to the data and the corresponding slopes are indicated.

distribution. As a result, the intensity ratio of these two peaks is sensitive to temperature [35]. Apparently, a temperature sensor can be made by monitoring the intensity ratio of these two PL peaks, which is defined as the thermometric parameter R [36,37]. Upon the excitation at 405 nm, the temperature-dependent R results are presented in Fig. 4 (a). It shows that R is mostly sub-linear with the surrounding temperature in the low temperature region (4 K $\leq T \leq$ 200 K). Previously, a prototype of temperature sensors had been advised in the use of fluorescence decay for Er-doped silicon, which operated over the range 40–150 K [22,38]. Note that a comparatively wider temperature range downwards to 4 K has been realized for our Er/O-doped silicon phosphors. By regression analysis of the data in Fig. 4 (a), the relationship between R and temperature (T) follows the equation below:

$$R = 0.474 + 0.00122T \quad (1)$$

Based on the curve in Fig. 4 (b), an activation energy of ~4.7 meV can be extracted. This fitted value is close to the actual energy difference between the first and second $^4I_{13/2}$ sublevels. The absolute sensitivity (S_a) is then given by $S_a = R\Delta E/kT^2$. As shown in Fig. 4 (c), it goes up steadily with a representative value of $\sim 11.7 \times 10^{-3}$ K^{-1} at 50 K as the temperature decreases from room temperature. These values even surpass the corresponding results obtained with erbium-doped glass sensors above room temperature [39]. In fact, by DC treatment, the nonradiative transition in our Er/O-doped silicon is negligible at low temperatures, exhibiting a near-unity internal quantum efficiency at 4 K, which makes it more suitable in the cryogenic temperature range [12]. As such, it is rational to deduce that the measurement principle on the basis of fluorescence ratiometric emission by Er/O-doped Si is feasible at cryogenic temperature.

The applicability of this fluorescence ratiometric strategy in thermal sensing was then demonstrated through the experimental scheme as depicted in Fig. 5 (a). The detailed description is presented in the section of Materials and methods. After being heated up to a certain temperature in Fig. 5 (b), the intensities of peaks 1 and 2 for the sample were measured and the corresponding R was calculated. By substituting R to equation (1) above, we derived the average temperature as well as the thermal sensing accuracy of Er/O-doped silicon as illustrated in Fig. 5 (c) and (d). The read-out temperature agrees well with the preset values

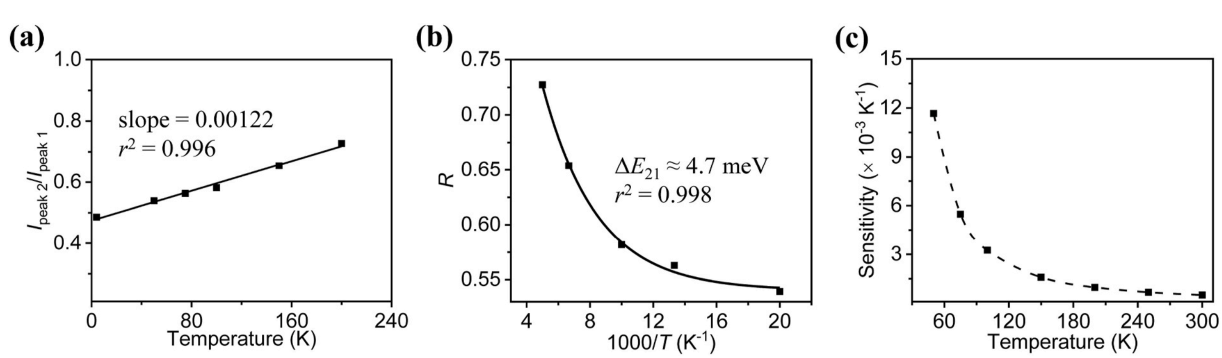

Fig. 4. (a) Fluorescence intensity ratio as a function of temperature. Fit of Eq. (1) to $R(T)$ is depicted as a solid line. (b) Arrhenius plot of intensity ratio vs. inversed temperature by $R = B\exp(-\Delta E_{21}/kT)$, where ΔE_{21} is the energy gap between the first and second coupled sublevels of $^4I_{13/2}$, B the proportionality constant, k the Boltzmann constant, and T the temperature of samples. The derived activation energy is then indicated. (c) Temperature sensitivity as a function of temperature. The dash line is a guide-to-the-eye.

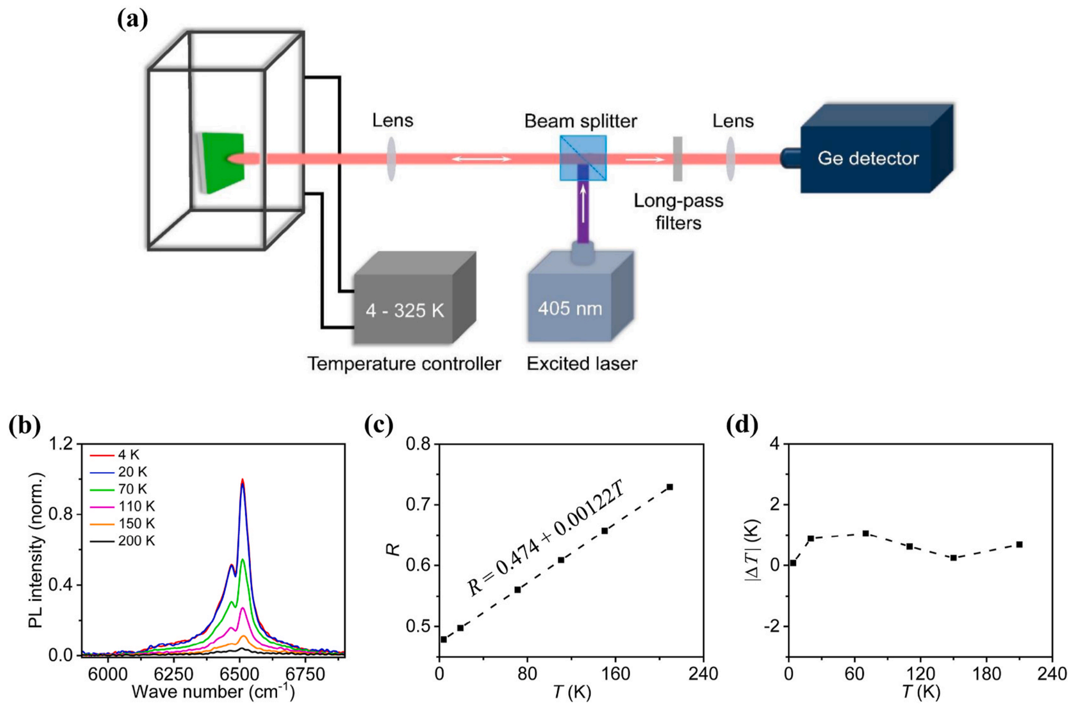

Fig. 5. (a) Schematic diagram of experimental setup for fluorescence ratiometirc thermometry. (b) Temperature-dependent emission spectra of Er/O-doped silicon phosphors. (c) Temperature read-out by using the linear equation derived from the regression analysis of R vs. T in (b). (d) Temperature accuracies ($|\Delta T|$) of the ratiometric thermometry based on Er/O-doped silicon phosphors.

with a high resolution less than 1.0 K. As these results were realized on our Er/O-doped silicon, the development of sensors and actuators is promising for fully integrated silicon photonics in the future.

4. Conclusion

In summary, a series of DC conditions such as annealing temperature and time, along with cooling rate, have been well defined to beef up the PL intensities of Er/O-doped silicon. The results revealed that annealing at 950 °C for 5 min, and then cooling down at a rate larger than −500 °C s^{-1} can boost the PL intensity, likely resulting from the more orderly Er distribution. In addition, co-doping of oxygen with an optimal O:Er ratio of ~2.5 can benefit Er radiation in crystalline silicon. A fluorescence ratiometric thermometry has been demonstrated by the thermal coupling of Er sublevels at communication wavelengths. This work may pave the way for developing fluorescent sensors in extreme environments based on rare-earth-doped silicon.

Author statement

This work was under the supervision of Yaping Dan. Huimin Wen carried out the experiment and wrote the first draft of the manuscript. Pu Zhang and Jin Hong contributed to the PL measurement and data analysis. Fangyu Yue and Jingquan Liu reviewed the manuscript and made some revisions. All authors read and contributed to the manuscript.

Declaration of competing interest

The authors declare that they have no known competing financial interests or personal relationships that could have appeared to influence the work reported in this paper.

Acknowledgements

We acknowledge the primary financial support from the National Science Foundation of China (22175112, 61874043, and 21703140), the special-key project of the "Innovative Research Plan", Shanghai Municipality Bureau of Education (2019-01-07-00-02-E00075), the Startup Fund for Young Faculty at Shanghai Jiao Tong University (SFYF at SJTU), and the Open Research Fund of Key Laboratory of Polar Materials and Devices, Ministry of Education.

References

[1] N. Margalit, C. Xiang, S.M. Bowers, A. Bjorlin, R. Blum, J.E. Bowers, Perspective on the future of silicon photonics and electronics, Appl. Phys. Lett. 118 (2021), 220501, https://doi.org/10.1063/5.0050117.
[2] D.-S. Liu, J. Wu, H. Xu, Z. Wang, Emerging light-emitting materials for photonic integration, Adv. Mater. 33 (2021), 2003733, https://doi.org/10.1002/adma.202003733.
[3] Q. Cheng, M. Bahadori, M. Glick, S. Rumley, K. Bergman, Recent advances in optical technologies for data centers: a review, Optica 5 (2018) 1354–1370, https://doi.org/10.1364/OTPICA.5.001354.
[4] Z. Wang, A. Abbasi, U. Dave, A. De Groote, S. Kumari, B. Kunert, C. Merckling, M. Pantouvaki, Y. Shi, B. Tian, K. Van Gasse, J. Verbist, R. Wang, W. Xie, J. Zhang, Y. Zhu, J. Bauwelinck, X. Yin, Z. Hens, J. Van Campenhout, B. Kuyken, R. Baets, G. Morthier, D. Van Thourhout, G. Roelkens, Novel light source integration approaches for silicon photonics, Laser Photon. Rev. 11 (2017), 1700063, https://doi.org/10.1002/lpor.201700063.
[5] Z. Zhou, B. Yin, J. Michel, On-chip light sources for silicon photonics, Light Sci. Appl. 4 (2015) e358, https://doi.org/10.1038/lsa.2015.131.
[6] J. Wang, Y. Long, On-chip silicon photonic signaling and processing: a review, Sci. Bull. 63 (2018) 1267–1310, https://doi.org/10.1016/j.scib.2018.05.038.
[7] H. Shen, D.-S. Li, D.-R. Yang, Research progress of silicon light source, Acta Phys. Sin. 64 (2015), 204208, https://doi.org/10.7498/aps.64.204208.
[8] N.Q. Vinh, N.N. Ha, T. Gregorkiewicz, Photonic properties of Er-doped crystalline silicon, Proc. IEEE 97 (2009) 1269–1283, https://doi.org/10.1109/JPROC.2009.2018220.
[9] A.J. Kenyon, Erbium in silicon, Semicond. Sci. Technol. 20 (2005) R65−R84, https://doi.org/10.1088/0268-1242/20/12/R02.
[10] G. Franzò, F. Priolo, S. Coffa, Understanding and control of the erbium non-radiative de-excitation process in silicon, J. Lumin. 80 (1998) 19–28, https://doi.org/10.1016/S0022-2313(98)00066-0.
[11] J. Hong, H. Wen, J. He, J. Liu, Y. Dan, J.W. Tomm, F. Yue, J. Chu, C. Duan, Stimulated emission at 1.54 μm from erbium/oxygen-doped silicon-based light-emitting diodes, Photon. Res. 9 (2021) 714–721, https://doi.org/10.1364/PR.417090.
[12] H. Wen, J. He, J. Hong, S. Jin, Z. Xu, H. Zhu, J. Liu, G. Sha, F. Yue, Y. Dan, Efficient Er/O-doped silicon light-emitting diodes at communication wavelength by deep

cooling, Adv. Opt. Mater. 8 (2020), 2000720, https://doi.org/10.1002/adom.202000720.

[13] M.A. Lourenço, M.M. Milošević, A. Gorin, R.M. Gwilliam, K.P. Homewood, Super-enhancement of 1.54 μm emission from erbium codoped with oxygen in silicon-on-insulator, Sci. Rep. 6 (2016), 37501, https://doi.org/10.1038/srep37501.

[14] B.A. Andreev, Z.F. Krasilnik, D.I. Kryzhkov, D.V. Shengurov, A.N. Yablonskiy, V. P. Kuznetsov, Luminescent properties of MBE-grown Si:Er/SOI structures, J. Lumin. 132 (2012) 3148–3150, https://doi.org/10.1016/j.jlumin.2011.11.025.

[15] A. Polman, Erbium implanted thin film photonic material, J. Appl. Phys. 82 (1997) 1–39, https://doi.org/10.1063/1.366265.

[16] S. Coffa, F. Priolo, G. Franzò, V. Bellani, A. Carnera, C. Spinella, Optical activation and excitation mechanisms of Er implanted in Si, Phys. Rev. B 48 (1993) 11782–11788, https://doi.org/10.1103/PhysRevB.48.11782.

[17] G.G. de Boo, C. Yin, M. Rančić, B.C. Johnson, J.C. McCallum, M.J. Sellars, S. Rogge, High-resolution spectroscopy of individual erbium ions in strong magnetic fields, Phys. Rev. B 201 (2020), 155309, https://doi.org/10.1103/PhysRevB.102.155309.

[18] K.V. Feklistov, D.S. Abramkin, V.I. Obodnikov, V.P. Popov, Doping silicon with erbium by recoil implantation, Tech. Phys. Lett. 41 (2015) 788–792, https://doi.org/10.1134/S1063785015080209.

[19] M. You, Z. Lin, X. Li, J. Liu, Chip-scale silicon ring resonators for cryogenic temperature sensing, J. Lightwave Technol. 38 (2020) 5768–5773, https://doi.org/10.1109/JLT.2020.3002552.

[20] S.A. Wade, S.F. Collins, G.W. Baxter, Fluorescence intensity ratio technique for optical fiber point temperature sensing, J. Appl. Phys. 94 (2003) 4743–4756, https://doi.org/10.1063/1.1606526.

[21] C.J. Yeager, S.S. Courts, A review of cryogenic thermometry and common temperature sensors, IEEE Sensor. J. 1 (2001) 352–360, https://doi.org/10.1109/7361.983476.

[22] A.K. Kewell, G.T. Reed, F. Namavar, Integrated temperature sensor in Er-doped silicon, Sens. Actuators A-Phys. 65 (1998) 160–164, https://doi.org/10.1016/S0924-4247(97)01699-3.

[23] J.F. Ziegler, J.P. Biersack, U. Littmark, The Stopping and Range of Ions in Matter, Pergamon, New York, 1985.

[24] J.F. Ziegler, SRIM-2013 Software Package, Available online at: http://www.srim.org.

[25] J. Hong, H. Wang, F. Yue, J.W. Tomm, D. Kruschke, C. Jing, S. Chen, Y. Chen, W. Hu, J. Chu, Emission kinetic from PbSe quantum dots in glass matrix at high excitation levels, Phys. Status Solidi Rapid Res. Lett. 12 (2018), 1800012, https://doi.org/10.1002/pssr.201800012.

[26] M. He, D. Yang, D. Li, Electroluminescence from metal-oxide-semiconductor devices based on erbium silicate nanocrystals and silicon nanocrystals co-embedded in silicon oxide thin films, J. Mater. Sci. Mater. Electron. 32 (2021) 20659–20667, https://doi.org/10.1007/s10854-021-06579-x.

[27] J. Michel, L.V.C. Assali, M.T. Morse, L.C. Kimerling, Erbium in silicon, Semiconduct. Semimet. 49 (1998) 111–156, https://doi.org/10.1016/S0080-8784(08)62502-8.

[28] D. Qi, S. Tang, L. Wang, S. Dai, X. Shen, C. Wang, S. Chen, Pulse laser-induced size-controllable and symmetrical ordering of single-crystal Si islands, Nanoscale 10 (2018) 8133–8138, https://doi.org/10.1039/C8NR00210J.

[29] D.J. Eaglesham, J. Michel, E.A. Fitzgerald, D.C. Jacobson, J.M. Poate, J.L. Benton, A. Polman, Y.-H. Xie, L.C. Kimerling, Microstructure of erbium-implanted Si, Appl. Phys. Lett. 58 (1991) 2797–2799, https://doi.org/10.1063/1.104739.

[30] M.A. Hughes, H. Li, N. Theodoropoulou, J.D. Carey, Optically modulated magnetic resonance of erbium implanted silicon, Sci. Rep. 9 (2019), 19031, https://doi.org/10.1038/s41598-019-55246-z.

[31] B. Zhang, Z. Wei, X. Wang, X. Fang, D. Wang, X. Gao, D. Fang, X. Wang, R. Chen, Effect of post thermal annealing on the optical properties of InP/ZnS quantum dot films, Nanoscale Res. Lett. 13 (2018) 369, https://doi.org/10.1186/s11671-018-2784-y.

[32] M. Ren, S.-S. Bao, R.A.S. Ferreira, L.-M. Zheng, L.D. Carlos, A layered erbium phosphonate in pseudo-D_{5h} symmetry exhibiting field-tunable magnetic relaxation and optical correlation, Chem. Commun. 50 (2014) 7621–7624, https://doi.org/10.1039/C4CC02085E.

[33] C.D.S. Brites, A. Millán, L.D. Carlos, Lanthanides in luminescent thermometry, Handb. Phys. Chem. Rare Earths 49 (2016) 339–427, https://doi.org/10.1016/bs.hpcre.2016.03.005.

[34] X. Wang, O.S. Wolfbeis, R.J. Meier, Luminescent probes and sensors for temperature, Chem. Soc. Rev. 42 (2013) 7834–7869, https://doi.org/10.1039/C3CS60102A.

[35] V. Lojpur, G. Nikolić, M.D. Dramićanin, Luminescence thermometry below room temperature via up-conversion emission of Y_2O_3:Yb^{3+},Er^{3+} nanophosphors, J. Appl. Phys. 115 (2014), 203106, https://doi.org/10.1063/1.4880158.

[36] S. Yu, J. Xu, X. Shang, W. Zheng, P. Huang, R. Li, D. Tu, X. Chen, A dual-excitation decoding strategy based on NIR hybrid nanocomposites for high-accuracy thermal sensing, Adv. Sci. 7 (2020), 2001589, https://doi.org/10.1002/advs.202001589.

[37] P. Gao, X. Li, Y. Gong, G. Shen, S. Zhang, L. Guan, Highly sensitive up-conversion phosphor for optical thermometry: $CaLaAl_3O_7$:Er^{3+}/Yb^{3+}, J. Rare Earths 37 (2019) 937–942, https://doi.org/10.1016/j.jre.2018.12.005.

[38] Z.Y. Zhang, T. Sun, K.T.V. Grattan, A.W. Palmer, Erbium-doped intrinsic fiber sensor for cryogenic temperature measurement, Sens. Actuators A-Phys. 71 (1998) 183–186, https://doi.org/10.1016/S0924-4247(98)00191-5.

[39] Y.K. Kshetri, T. Kamiyama, S. Torii, S.H. Jeong, T.-H. Kim, H. Choi, J. Zhou, Y. P. Feng, S.W. Lee, Electronic structure, thermodynamic stability and high-temperature sensing properties of Er-α-SiAlON ceramics, Sci. Rep. 10 (2020) 4952, https://doi.org/10.1038/s41598-020-61105-z.